Electric Machines & Power Systems

ISSN: 0731-356X (Print) (Online) Journal homepage: http://www.tandfonline.com/loi/uemp19

STEADY-STATE ANALYSIS OF AN INDUCTION GENERATOR SELF-EXCITED BY A CAPACITOR IN PARALLEL WITH A SATURABLE REACTOR

S. M. ALGHUWAINEM

STEADY-STATE ANALYSIS OF AN INDUCTION GENERATOR SELF-EXCITED BY A CAPACITOR IN PARALLEL WITH A SATURABLE REACTOR

S. M. ALGHUWAINEM

Department of Electrical Engineering
King Saud University
P.O. Box 800, Riyadh, Saudi Arabia 11421

ABSTRACT

Poor voltage regulation is one of the major drawbacks of an isolated self-excited induction generator. The terminal voltage may increase considerably due to a small increase in speed. In most developing countries, unregulated wind-turbines are often used due to their lower cost. Under these conditions the terminal voltage may increase to a dangerously high level which may cause damage to the machine, load or excitation capacitor. This paper examines the advantage of connecting a saturable reactor in parallel with the excitation capacitor. It is found that the saturable reactor improves voltage regulation considerably.

Keywords:- Induction Generators, Self-Excitation, Saturable Reactors.

List of Symbols:

f	Per-unit stator frequency = stator frequency / base frequency
ω	Per-unit rotor speed = rotor speed / synchronous speed
R_s, R_r, R_L	Stator, referred rotor and load resistance
X_s, X_r, X_c	Stator, referred rotor, and excitation capacitor reactance at base frequency
X_m, X_L	Machine and saturable reactor magnetizing reactance at base frequency
V_g, V_t	Air-gap and terminal voltage

Request reprints from S. M. Alghuwainem. Manuscript received in final form January 29, 1997.

0731-356X / 98 $12.00 + .00

1 INTRODUCTION

The growing concerns about the rapid depletion of fossil-fuel resources and the global movements for clean environments have accelerated the research and development of energy systems using renewable energy sources such as wind. The self-excited induction generator (SEIG) has been discussed in the literature [1-9] as a very suitable candidate for this type of application due to its low cost, simplicity, ruggedness, brushless rotor, and ease of maintenance, etc. The SEIG is essentially a three-phase induction machine with an external capacitor connected to its stator terminals while its shaft is driven by a prime-mover. In this case, the capacitor provides the lagging magnetizing reactive power which is necessary to establish the air-gap flux.

Unless the SEIG is connected to a utility grid, its frequency and stator voltage are free to vary with rotor speed and load. In most developing countries, the speed of a wind or micro-hydro turbine is not regulated in order to reduce the overall system cost. It is well known that capacitive requirement of an isolated SEIG is inversely proportional to speed, and hence the terminal voltage of an unregulated SEIG, with a fixed excitation capacitance, may increase considerably due to a small increase in speed [4, 5]. Capacitor failure at windfarms due to fluctuations in speed has been reported in the literature [6, 7]. This paper examines the advantage of connecting a saturable reactor in parallel with the excitation capacitor to improve voltage regulation. As the reactor saturates it absorbs the excess reactive power in the system due to the increase in speed, and thus prevents any further increase in the terminal voltage.

It is well known that the air-gap voltage of an isolated SEIG is limited by the saturation of the machine's magnetic circuit which makes the analysis of the SEIG's equivalent circuit inherently a nonlinear problem. By connecting a saturable reactor to the SEIG's terminal, an additional nonlinearity is introduced which complicates the analysis considerably. The previously published methods [1-9] assume no saturable reactor is present and hence the only nonlinearity is the machine's magnetizing reactance which is nonlinearly dependent on the machine's air-gap voltage.

In this paper, a shunt saturable reactor is included, whose reactance is nonlinearly dependent on the machine's terminal voltage. Therefore, two nonlinearities coexist which are coupled through the two node voltages, namely the air-gap voltage and the terminal voltage which are considered as two unknowns. The resulting equations are solved directly using a simple Mathcad [10] program on a personal computer. The calculated results are verified experimentally for a model system under a variety of test conditions.

2 SYSTEM MODELLING

The system consists of a 3-phase induction machine, which is being driven at a constant speed ω by a prime-mover. A balanced 3-phase excitation capacitor C, a resistive load (R_L) and a saturable reactor (X_L) are connected to the stator terminals. The steady-state equivalent circuit of the SEIG in this case is shown in Fig. 1.

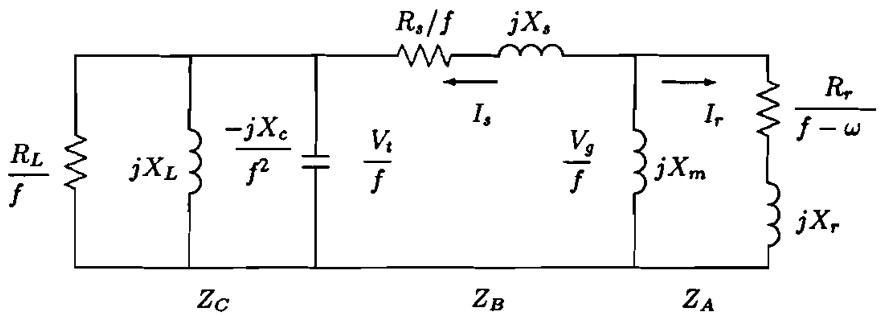

FIGURE 1 Per-phase equivalent circuit of the SEIG

All circuit parameters in Fig. 1 are assumed constant except the machine's magnetizing reactance X_m, the saturable reactance X_L, and the stator frequency f. It should be noted that X_m and X_L are dependent on the two node voltages V_g and V_t respectively through their respective magnetization characteristics. Therefore, the three unknowns may alternatively be taken as f, V_g and V_t.

For specified values of speed, excitation capacitance, machine and load parameters, it is generally possible to solve the circuit of Fig. 1 such that the self-excitation condition is satisfied. At self-excitation the total loop impedance (or total node admittance) at the machine's magnetizing node is zero. Therefore,

$$Z_A + Z_B + Z_C = 0 \tag{1}$$

It should be noted that these impedances are functions of the unknown variables f, V_g and V_t. Moreover, the two node voltages V_g and V_t are related by

$$V_t = \frac{Z_C}{Z_B + Z_C} V_g \tag{2}$$

The impedances Z_A, Z_B and Z_C from Fig. 1 are given by

$$Z_A = \frac{jX_m[R_r/(f-\omega) + jX_r]}{R_r/(f-\omega) + j(X_r + jX_m)} \tag{3}$$

$$Z_B = \frac{R_s}{f} + jX_s \tag{4}$$

$$Z_C = 1/[\frac{1}{jX_L} + \frac{f^2}{-jX_c} + \frac{f}{R_L}] \tag{5}$$

The previously published methods [1-9] regard X_L as constant (no saturable reactor), and hence the only unknowns are f and V_g, and hence equation (2) is not necessary. Equation (1) is then separated into real and imaginary parts which are equated to zero and solved using a gradient method such as the Newton-Raphson method.

In this paper, the reactance of the saturable reactor, X_L is assumed to vary with the terminal voltage V_t according to the reactor's magnetic circuit characteristics. Therefore, V_t must be taken as an independent variable, and hence, the unknowns are taken as f, V_g and V_t. Equations (1) and (2) are solved simultaneously for the three unknowns, using Mathcad [10] which is capable of solving a system of nonlinear equations with complex coefficients.

3 EXPERIMENTAL VERIFICATION

A model system consisting of a 380-V, 4-pole, 60-Hz, 2.9-A, Y-connected wound rotor induction machine, coupled to a variable speed dc motor drive was tested in the laboratory. The induction machine has the following per-unit measured parameters:-
$R_s = 0.092$, $R_r = 0.064$, $X_s = X_r = 0.21$. Its magnetizing reactance is given by

$$X_m(V_g) = 3.46 - 6.5V_g + 9.51V_g^2 - 4.77V_g^3 \tag{6}$$

where V_g is the air-gap open-circuit voltage. A 3-phase, Y-connected, balanced excitation capacitor and a saturable reactor are connected across the stator terminals. The saturable reactor is represented by the following reactance

$$X_L(V_t) = 66.45 + 116.93V_t - 257.98V_t^2 + 98.5V_t^3 \tag{7}$$

where V_t is the terminal voltage. Equations (6) and (7) are obtained using regression analysis on the magnetization characteristics test data of the machine and reactor respectively. Fig. 2 displays the variation of X_m and X_L with V_g and V_t respectively.

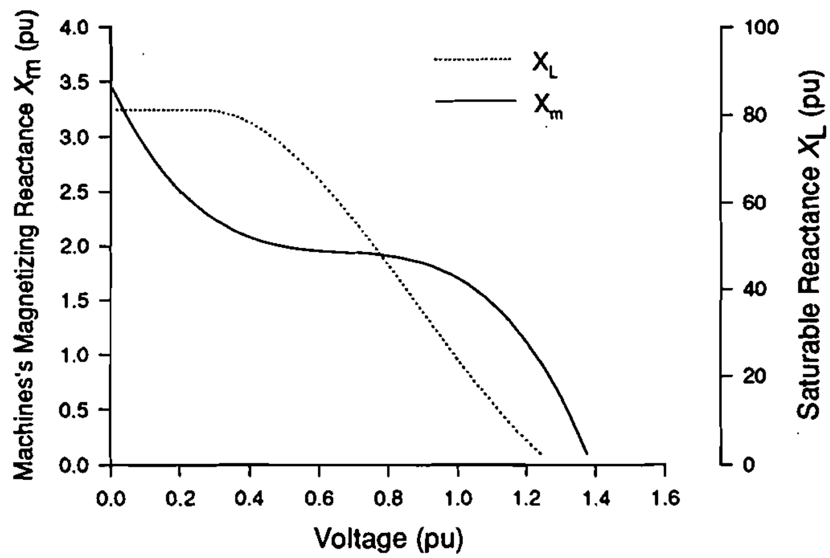

FIGURE 2 Variation of X_m and X_L with air-gap voltage and terminal voltage respectively.

Fig. 3 shows the calculated and measured variations of the terminal voltage, stator current and frequency, with speed, at no-load, and excitation capacitance $C = 25.5\mu F$. It is clear from Fig. 3, that a very good agreement exists between measured and calculated values, which verifies the accuracy of the proposed technique.

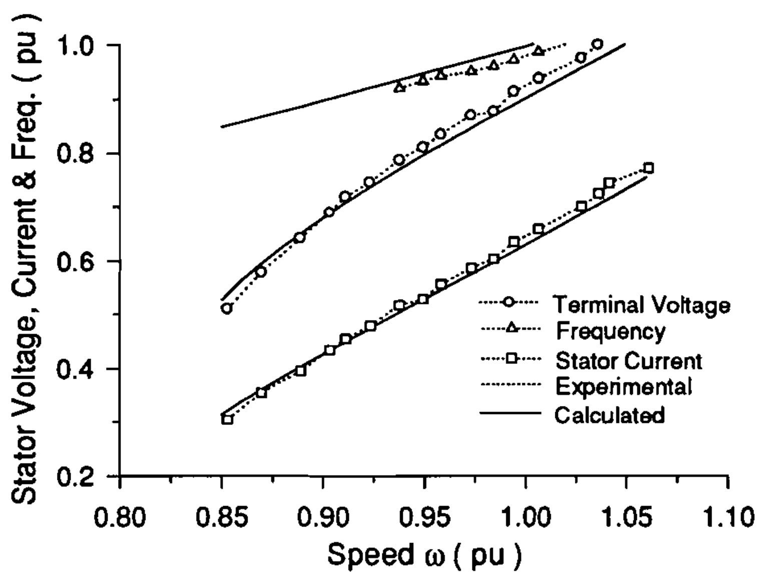

FIGURE 3 Variation of terminal voltage, stator current and frequency with speed at no-load, and $C = 25.5\mu F$.

4 EFFECT OF REACTOR SATURATION

Fig. 4 displays variation of the terminal voltage with speed while the excitation capacitance is kept constant at $C = 30\mu F$. It is clear from Fig. 4 that, without saturable reactor, the terminal voltage increases almost linearly with speed, in the region from V_t = 1 pu to V_t = 1.6 pu. However, with the saturable reactor the terminal voltage does not increase higher than V_t = 1.2 pu, which is the saturation voltage of the reactor. Fig. 5 shows variation of the terminal voltage with the excitation capacitance while speed is kept constant at $\omega = 1$ pu. It is clear from Fig. 5 that, without saturable reactor, the terminal voltage increases almost linearly with capacitance, in the region from V_t = 1 pu to V_t = 1.6 pu. However, with the saturable reactor the terminal voltage does not increase higher than V_t = 1.2 pu. By proper design of the saturable reactor magnetic circuit, it is possible to select the desired saturation voltage level at which the SEIG terminal voltage will remain constant.

5 EFFECT OF LOAD IMPEDANCE

The load impedance has a significant influence on the operating point of an isolated SEIG since it is directly in parallel with the excitation capacitance. The load power-factor is specially important since it affects the overall capacitive reactance.

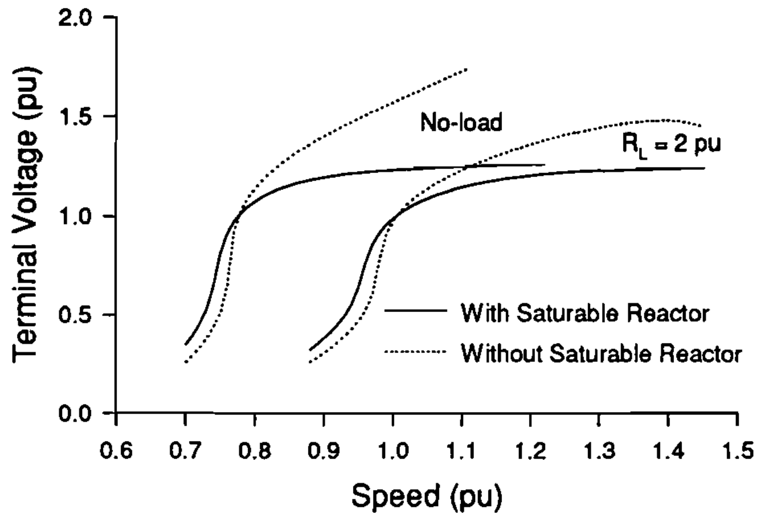

FIGURE 4 Variation of the terminal voltage with speed for constant excitation capacitance $C = 30\ \mu F$.

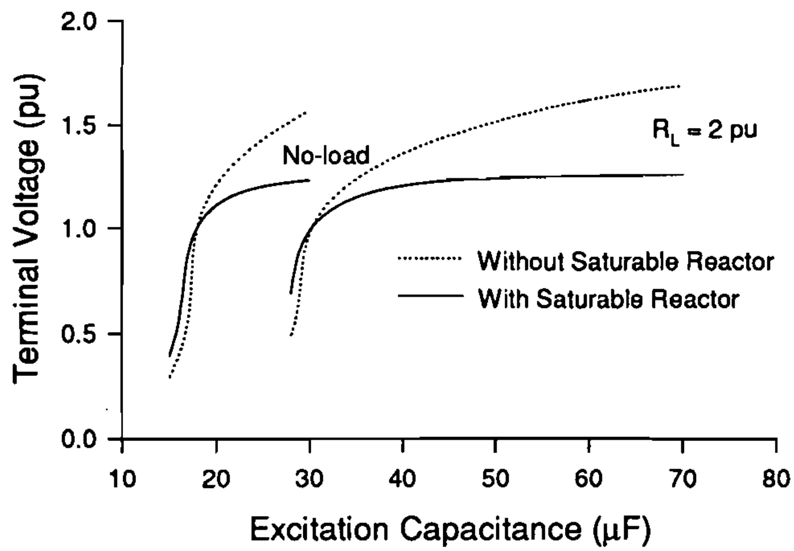

FIGURE 5 Variation of the terminal voltage with excitation capacitance at constant speed $\omega = 1$ pu.

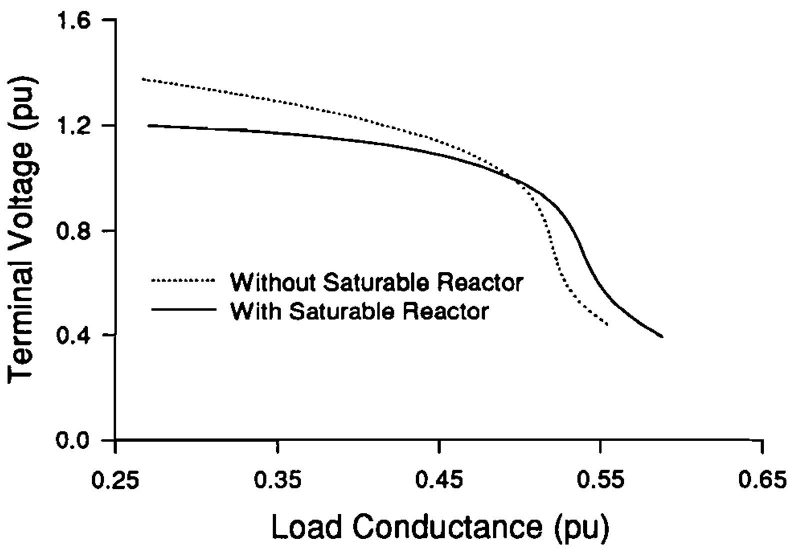

FIGURE 6 Variation of the terminal voltage with load conductance for resistive load, ω = 1 pu, $C = 30\ \mu F$.

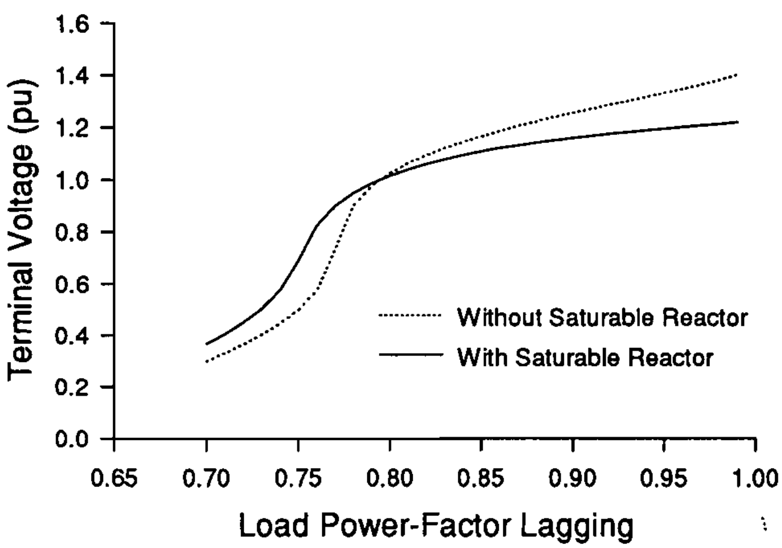

FIGURE 7 Variation of the terminal voltage with lagging load power-factor for $\omega = 1$ pu, $C = 45\ \mu F$.

Fig. 6 shows variation of the terminal voltage with load conductance for a pure resistive load. It is clear that the saturable reactor improves voltage regulation due to resistive load variation. Fig. 7 shows the effect of load power-factor on the terminal voltage, for constant load resistance, speed, and excitation capacitance. It is clear that the saturable reactor improves voltage regulation due to change in load power-factor.

6 CONCLUSIONS

In this paper, the advantages of connecting a shunt saturable reactor to the terminals of an isolated self-excited induction generator are highlighted. These advantages include improved voltage regulation and protection against over-voltages which are the major cause of excitation capacitor failure at wind farms which use unregulated wind-turbines. The presence of the saturable reactor will also protect against over-voltages caused by increase in capacitance. Capacitance is normally increased in order to compensate for voltage drop due to increased load current, but a large increase in capacitance may lead to over-excitation and hence over-voltage. The additional nonlinearity introduced by the saturable reactor complicates the analysis of the SEIG considerably. A method to analyze the steady-state performance characteristics of the SEIG with two nonlinearities is presented.

REFERENCES

[1] B. C. Doxy, "Theory and Application of the Capacitor-Excited Induction Generator," *The Engineer*, Vol. 216, 1963, pp. 893-897.

[2] G. Raina and O. P. Malik, "Wind Energy Conversion Using a Self-Excited Induction Generator," *IEEE Trans. on Power App. & Sys.*, Vol. 102, No. 12, 1983, pp. 3933-3936.

[3] L. Ouazene and G. McPherson, Jr., "Analysis of the Isolated Induction Generator," *IEEE Trans. on Power App. & Sys.*, Vol. 102, No. 8, 1983, pp. 2793-2798.

[4] N. H. Malik and A. H. Al-Bahrani, "Influence of the Terminal Capacitor on the Performance Characteristics of a Self-Excited Induction Generator," *IEE Proceedings-C*, Vol. 137, No. 2, 1990, pp. 168-173.

[5] A. K. Al Jabri and A. I. Alolah, "Limits on the Performance of of Three-Phase Self-Excited Induction Generators," *IEEE Trans. on Energy Conversion*, Vol. 5, No. 2, 1990, pp. 350-356.

[6] L. Tang and R. Zavadil, "Shunt Capacitor Failures Due to Windfarm Induction Generator Self-Excitation Phenomenon," *IEEE Trans. on Energy Conversion*, vol. 8, No. 3, 1993 pp. 513-519.

[7] J. C. Smith, J. I. Herrera and M. F. McGranaghan, "Analysis of Capacitor Failure at the Kamoa Windfarm on the Island of Hawaii," *Solar Energy Research Institute*, (SERI, now known as NREL), August 1989.

[8] S. M. Alghuwainem, "Performance analysis of a PV powered dc motor driving a 3-phase self-excited induction generator," *IEEE Trans. on Energy Conversion*, vol. 11, no. 1, March 1996, pp. 155-161.

[9] S. M. Alghuwainem, "Speed Control of a PV Powered DC Motor Driving a Self-Excited 3-Phase Induction Generator for Maximum Utilization Efficiency," *IEEE PES* Summer Meeting, July 28 - August 1, 1996, Denver, Colorado, Paper 96 SM 570-2 EC.

[10] MathSoft Inc., "Mathcad User's Guide," Cambridge, Massachusetts, 1994.

Appendix

Program Listing

a) Define all constants:

$R_s := 0.092$ $\quad R_r := 0.064$
$X_s := 0.210$ $\quad X_r := 0.210$
$R_L := 10^{22}$ $\quad \omega := 1.00$
$X_c := 1.37$

b) Define X_m and X_L in terms of V_g and V_t:

$$X_m(V_g) := 3.46 - 6.5V_g + 9.51V_g^2 - 4.77V_g^3$$

$$X_L(V_t) := 66.45 + 116.93V_t - 257.98V_t^2 + 98.5V_t^3$$

c) Define Z_A to Z_C as functions of the unknowns:

$$Z_A(f, V_g) = \frac{jX_m(V_g)[R_r/(f-\omega) + jX_r]}{R_r/(f-\omega) + j(X_r + jX_m(V_g))}$$

$$Z_B(f) = \frac{R_s}{f} + jX_s$$

$$Z_C(f, V_t) = 1/[\frac{1}{jX_L(V_t)} + \frac{f^2}{-jX_c} + \frac{f}{R_L}]$$

d) Solve using the built-in "GIVEN-FIND" procedure:

GIVEN

$$Z_A(f, V_g) + Z_B(f) + Z_C(f, V_t) = 0$$

$$\left|\frac{Z_C(V_t, f)}{Z_B(f) + Z_C(V_t, f)}\right| V_g - V_t = 0$$

FIND (f, V_g, V_t)